Petrogenetic linkages among fO_2, isotopic enrichments-depletions and crystallization history in martian basalts. Evidence from the distribution of phosphorus and vanadium valance state in olivine megacrysts. C.K. Shearer[1], P.M. Aaron[1], P.V. Burger[1], Y. Guan[2], A.S. Bell[1], J.J. Papike[1], and S.R. Sutton[3,4]. [1]Institute of Meteoritics, University of New Mexico, Albuquerque, New Mexico 87131 (cshearer@unm.edu), [2] Division of Geological and Planetary Sciences, California Institute of Technology, Pasadena, California, [3]Department of Geophysical Sciences, University of Chicago, Chicago, Illinois 60637. [4]Center for Advanced Radiation Sources, University of Chicago, Chicago, Illinois 60637

Introduction: A prominent geochemical feature of the shergottites is the large range in initial Sr isotopic ratios and initial ε^{Nd} values. Associated with this geochemical characteristic of this suite of martian basalts is a fairly systematic variation in oxygen fugacity. The depleted olivine-phyric shergottites are commonly reduced (~IW+1) and exhibit limited variation in fO_2 during crystallization, whereas the enriched olivine-phyric shergottites are more oxidized and exhibit a substantial variation in fO_2 during crystallization (~IW+1 to FMQ+0.7). Interpreting the relationship between isotopic-geochemical characteristics of these basalts and intensive variables such as fO_2 is fundamental to deciphering the origin of olivine megacrysts in the shergottites, the petrogenesis of martian magmatism, and the nature of the martian mantle. Our study focuses upon deciphering the micro-scale crystallization history of olivine megacrysts using changes in the redox state during crystallization and linking it to micro-scale changes in P. Reconstructing the crystallization history of the olivine is necessary in order to evaluate the validity of the various models explaining the origin of the isotopic and geochemical-signatures that are observed in the shergottites. This has fundamental implications for the fO_2 of the martian mantle and the origin and nature of the enriched component in the "enriched" shergottites.

Analytical Approach: Olivine-phyric shergottites Yamato 980459 (Y98) and Northwest Africa 1183 (NWA 1183) were selected for this this study because they represent depleted and enriched olivine-phyric shergottites, respectively. In addition, we conducted experiments on Y98 bulk compositions and examined the Y98 charges that were held above the liquidus at 1500 °C at oxygen fugacities of IW-1, IW+1, and IW+3.5 (≈QFM) for 24 h to allow homogenization and equilibration with the gas mixture, then lowered to the desired final quench temperature (1320 or 1375–1380°C) at 100 °C/h, held for 48 h, then drop quenched into deionized water.

Samples and experiments were imaged and analyzed using the electron microprobe (EPMA), secondary ion mass spectrometry (SIMS) and nanoSIMS. Samples were initially characterized using backscattered electron imaging (BSE) using the JEOL 8200 EPMA in the Department of Earth and Planetary Sciences at the University of New Mexico. Suitable grains were chosen for WDS mapping. Two sets of x-ray maps were collected: major and minor element maps for Cr, Mn, Mg, Fe, and Ca were produced with a beam current of 100 nA while minor element maps for Cr, V, P, and Ti were produced with a beam current of 500 nA, using a spot size of <1 micron, an accelerating voltage of 15kV, a dwell time of 700 ms, and pixel dimensions of 450 x 450. The minor element x-ray mapping followed the methodology of [1-3]. The x-ray maps were used to position traverses for quantitative analysis of the major, minor, and trace elements. Aluminum, Fe, Mg, Si, Ti, Na, Mn, Cr, Ca, P, V, and Ni were analyzed by electron microprobe at a beam current of 20 nA, using a <1 micron spot, and a 15kV accelerating voltage. The olivine grains were further analyzed by nanoSIMS with a 2x2 μm O^- beam of ~300 nA and 12 KeV impact energy. Analyses were taken every 3 to 5 μm depending on the scale of the phosphorus zoning. Approximately 300 trace element analyses were performed on the olivines. Secondary ions of ^{27}Al, ^{28}Si, ^{47}Ti, ^{51}V, ^{59}Co, ^{62}Ni and ^{89}Y were simultaneously collected with electron multipliers (EMs) at high mass resolution. For every analysis point in standards and unknowns, the intensities for each mass were normalized to ^{28}Si and multiplied to the wt. % SiO_2. Calibration curves were constructed using these values for the standards (UNM ion probe standards for olivine, and pyroxene) versus concentration. These calibration curves were then used to calculate concentrations in the olivines from the two martian basalts. To cross check nanoSIMS analyses, we conducted additional SIMS analyses in the more homogeneous regions of the martian olivines using the Cameca ims 4f at the University of New Mexico.

X-Ray absorption near-edge spectroscopic (XANES) analyses of V valance state in natural olivine and experiments will be performed with the GeoSoilEnviroCARS (GSECARS) X-ray microprobe at the Advanced Photon Source (APS), Argonne National Laboratory, IL following the approach of Sutton et al. [4] and Karner et al. [5].

Observations: Comparisons between reduced, depleted shergottite (Y98) and an oxidized, enriched shergottite (NWA1183) indicate differences in the crystallization history of the olivine megacrysts (Fig. 1).

Phosphorus concentrations in the olivine from these two basalts range from less than 0.02 to up to approximately 0.70 wt. % P_2O_5. The olivine megacrysts in Y98 appear to exhibit three episodes of growth as defined by P zoning: (1) an absorbed P- and Ti-rich xenocrystic core, (2) an intermediate region consisting of continuous, oscillatory P zoning, and (3) an outer rim consisting of discontinuous, oscillatory P zoning. The olivine megacrysts in NWA1183 appear to exhibit three episodes of growth defined by P zoning: (1) a euhedral core surrounded by oscillatory P zoning, (2) an intermediate region consisting of continuous, oscillatory P zoning, and (3) an outer rim consisting of discontinuous, oscillatory P zoning. The P in the olivine reflects subtle, but real differences in the P content of different shergottite melts (Y98 xenocrystic core, outer portion of the Y98 megacryst, and NWA1183 megacryst), incompatible element behavior of P during olivine crystallization, and solute trapping during episodes of rapid olivine growth. Although P should behave incompatibly in basaltic systems, there is little relationship between isotopic characteristics and P content in the enriched-depleted shergottites. This observation may indicate that the P content of the basalts was buffered by a phase in the martian mantle that was not entirely consumed during partial melting. Aluminum in the olivine is generally correlated with P enrichment in the olivine and reflects a coupled substitution of P-Al into olivine tetrahedral and octahedral sites during periods of rapid olivine growth. On the other hand, V is not correlated with P in Y98, but correlated with P in many of the oscillatory zones in NWA1183 (Fig. 2). The change in correlation to P may reflect changes in V valance state (V^{3+}, V^{4+} and V^{5+}) during olivine crystallization. Within the crystallization histories defined by the P zoning in olivine, the calculated fO_2 remains fairly constant at ~IW+1 for Y98, but changes dramatically for NWA1183 from olivine core to the oscillatory zones and rim (~IW+1.8 to FMQ+0.5). Although we cannot preclude the mixing of reduced and oxidized components (magma mixing, mixing of early olvine+chromite+pyroxene xenocrysts), numerous lines of evidence suggest that the changes in fO_2 during olivine crystallization may reflect auto-oxidation due to degassing of the NWA1183 magma prior to eruption. These observations suggest a limited variation in the fO_2 of the martian mantle (IW to IW+1), that enriched and depleted sources for the shergottites reside in the mantle, and that magmas produced in these sources have different capabilities for changing their redox state during crystallization. The latter may reflect differences in the character and composition of the volatile component of the enriched and depleted sources for the shergottites.

References: [1] Milman-Barris, M. et al. (2008) Contributions *to Mineralogy and Petrology*, doi: 10.1007/s00410-007-0268-7. [2] McCanta, M.C. et al (2008) *Lunar and Planetary Science.* Houston: Lunar Planetary Institute, 208. Abstract #1807. [3] Stolper, E.M. et al. (2009) *Joint Assembly Supplement.* Toronto, American Geophysical Union. Abstract #V74B-01. [4] Sutton, S.R. et al. (2005) *Geochimica et Cosmochimica Acta* 69, 2333–2348. [5] Karner, J. et al. (2006) *American Mineralogist* 91, 270–277.

Figure 1. BSE and x-ray maps of A. Y98 and B. NWA1183.

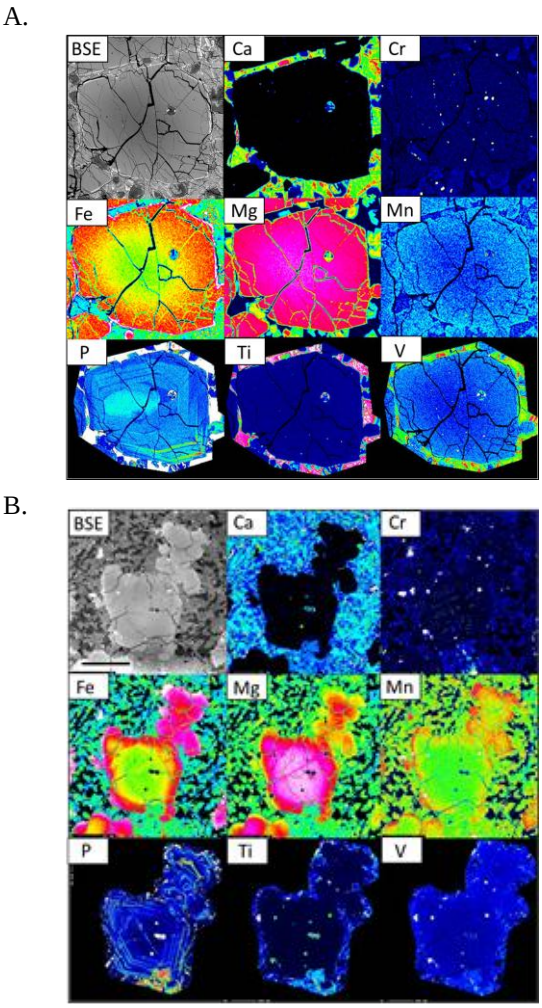

Figure 2. Microprobe and nanoSIMS traverses across A.Y98 and B.NWA1183.